Structural Engineering and Mechanics, Vol. 15, No. 6 (2003) 735-752
DOI: http://dx.doi.org/10.12989/sem.2003.15.6.735

The mixed finite element for quasi-static and dynamic analysis of viscoelastic circular beams

Fethi Kadıoğlu† and A. Yalçın Aköz‡

Faculty of Civil Engineering, Istanbul Technical University, 80626 Maslak-Istanbul, Turkey

(Received January 5, 2002, Accepted April 8, 2003)

Abstract. The quasi-static and dynamic responses of a linear viscoelastic circular beam on Winkler foundation are studied numerically by using the mixed finite element method in transformed Laplace-Carson space. This element VCR12 has 12 independent variables. The solution is obtained in transformed space and Schapery, Dubner, Durbin and Maximum Degree of Precision (MDOP) transform techniques are employed for numerical inversion. The performance of the method is presented by several quasi-static and dynamic example problems.

Key words: viscoelastic circular beam; mixed finite element; inverse Laplace transform; elastic foundation.

1. Introduction

The circular structures received considerable interest due to their wide application in engineering usage. The beam on elastic foundation for elastic case has been treated by various authors. In these investigations, closed form solution of differential equations are given and numerical results have been tabulated for special cases (Hetenyi 1946, Miranda and Nair 1966, Ting and Mockry 1983). Aköz *et al.* (1991) developed a mixed finite element for elastic three-dimensional bars using Gâteaux differential. Using similar approach, Aköz and Kadıoğlu (1996) has studied circular beams on elastic foundation.

Viscoelastic constitutive relation is more realistic than the elastic constitutive relation to reflect the material behaviour. Some more information about viscoelasticity can be found in literature (Flügge 1975, Christensen 1982). Although the calculation by viscoelastic theory is more complex than the elastic theory, viscoelastic theory gives more realistic result. Various methods have been developed to analyse of viscoelastic problems.

Satisfying some requirements, the problem of viscoelastic structures can be solved as elastic structure, employing correspondence principle (Findley *et al.* 1976). The Laplace and Fourier transform methods have been widely used in solution of viscoelastic problems (Rabbatnow 1980). The problems have complex geometry and constitutive relations, closed form solution are often not possible and numerical techniques should be employed. The applications of the numerical methods

† Doctor
‡ Professor

to viscoelastic problems have been presented by numerous authors: White (1986) applied the time interval form finite difference method to perform a finite element analysis in a quasi-static problem. Addey and Brebbia (1973) used an approximate inversion procedure to obtain the inversion solution of associated elastic problem. Johnson *et al.* (1997) derived the elastodynamic equations of motion for thick viscoelastic beams. Chen (1995) and Wang *et al.* (1997) studied the linear viscoelastic Timoshenko beam for quasi-static and dynamic response. Chen (1995) assumed that Poisson ratio ν is constant and only elasticity modulus is viscoelastic. The relaxation modulus is expressed by the same Prony Series for both normal stress-strain and shear stress-strain relations. He selected the nodal variables as v, ω the displacement and rotation of cross-section respectively. The hybrid method was used to remove the time parameter using the Laplace transform and associated equation is solved using finite element method. Chen (1995) used Hamilton's variational principle to obtain finite element. To obtain the actual displacement in the time domain, the numerical inversion of Laplace transform method of Hanig and Hirdes was used by Chen (1995). Kadıoğlu (1999), Aköz and Kadıoğlu (1999) also studied Timoshenko and Euler-Bernouili beam that has the general forms of relaxation modulus for both Poisson ratio and Young modulus for quasi-static and dynamic response. The Gâteaux differential approaches is employed to construct the functional. In order to remove the time derivatives from the governing equations, the method of the Laplace-Carson transform was utilized. Two mixed finite element formulations TB12 and TB4 were derived in the transformed space. For the inverse transform Schapery and Fourier method were used.

In this study, the viscoelastic circular beam on elastic foundation is analysed for quasi-static and dynamic responses. In order to remove the time derivatives from the governing equations and boundary conditions, the method of the Laplace-Carson transform is utilized. The special attention is given to the numerical inverse of Laplace transform. The available numerical inverse transform methods; such as Shapery, Fourier, Durbin, Dubner, Maximum Degree of Presicion (MDOP) are used to solve the same problems and results are compared and disscussed in the applications. For more information reader may be consulted to the literature (Kadıoğlu 1999).

2. The field equations

For a circular beam loaded by the external loads perpendicular to the plane of the structure, effective internal force components are depicted in Fig. 1.

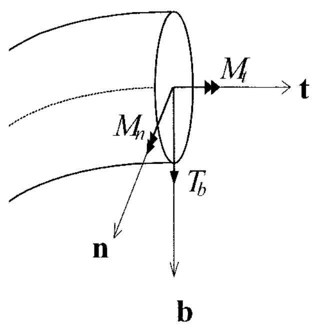

Fig. 1 Internal forces

The equilibrium equations and kinematic equations can be obtained from literature as follows (Aköz and Kadıoğlu 1996)

$$
\begin{aligned}
&-\frac{dT_b}{d\theta}-qR+kRu_b = 0 \\
&-\frac{dM_n}{d\theta}-M_t+RT_b-Rm_n = 0 \qquad \text{equilibrium equations} \\
&-\frac{dM_t}{d\theta}+M_n-Rm_t+k_tR\Omega_t = 0
\end{aligned} \tag{1}
$$

$$
\begin{aligned}
&\frac{d\Omega_t}{d\theta}-\Omega_n-R\omega_t = 0 \\
&\frac{d\Omega_n}{d\theta}+\Omega_t-R\omega_n = 0 \qquad \text{kinematic equations} \\
&\frac{du_b}{d\theta}+R\Omega_n-R\gamma_b = 0
\end{aligned} \tag{2}
$$

The stress-strain relations for viscoelastic materials can be written in hereditary form as (Rabbatnow 1980)

$$
\begin{aligned}
\sigma_{(t)} &= Y_{(0)}\varepsilon_{(t)}+\int_0^t \frac{dY_{(t-\tau)}}{d(t-\tau)}\varepsilon_{(\tau)}d\tau \\
\tau_{(t)} &= Y_{1(0)}\gamma_{(t)}+\int_0^t \frac{dY_{1(t-\tau)}}{d(t-\tau)}\gamma_{(\tau)}d\tau
\end{aligned} \tag{3}
$$

where $Y_{(t)}$ and $Y_{1(t)}$ are relaxation moduli for normal and shear stresses respectively. The inverse relations can be written as follows:

$$
\begin{aligned}
\varepsilon_{(t)} &= J_{(0)}\sigma_{(t)}+\int_0^t \frac{dJ(t-\tau)}{d(t-\tau)}\sigma_{(\tau)}d\tau \\
\gamma_{(t)} &= J_{1(0)}\tau_{(t)}+\int_0^t \frac{dJ_{1(t-\tau)}}{d(t-\tau)}\tau_{(\tau)}d\tau
\end{aligned} \tag{4}
$$

where $J_{(t)}$ and $J_{1(t)}$ are creep moduli. Taking into account well-known equations for the kinematics of the beam, for bending, torsion and shear and using constitutive Eq. (3) and equilibrium equations we obtain bending, torsion and shear rigidity as follows:

$$
\begin{aligned}
M_{n(t)} &= I_n\left\{Y_{(0)}\omega_{(\tau)}+\int_0^t \frac{dY_{(t-\tau)}}{d(t-\tau)}\omega_{n(\tau)}d\tau\right\} \\
M_{t(t)} &= I_0\left\{Y_{1(0)}\omega_{(t)}+\int_0^t \frac{dY_{1(t-\tau)}}{d(t-\tau)}\omega_{t(\tau)}d\tau\right\}
\end{aligned}
$$

$$T_{b(t)} = k'A\left\{Y_{1(0)}\gamma_{(t)} + \int_0^t \frac{dY_{1(t-\tau)}}{d(t-\tau)}\gamma_{(\tau)}d\tau\right\} \tag{5}$$

The above relations can be written in simple forms using three operators:

$$\begin{aligned} -M_n + D_n^*\omega_n &= 0 \\ -M_t + D_t^*\omega_t &= 0 \\ -T_b + H^*\gamma_b &= 0 \end{aligned} \tag{6}$$

where D_n^*, D_t^* and H^* are defined as

$$\begin{aligned} D_n^* f &= I_n\left\{Y_{(0)}f_{(t)} + \int_0^t \frac{dY_{(t-\tau)}}{d(t-\tau)}f_{(\tau)}d\tau\right\} \\ D_t^* f &= I_0\left\{Y_{1(0)}f_{(t)} + \int_0^t \frac{dY_{1(t-\tau)}}{d(t-\tau)}f_{(\tau)}d\tau\right\} \\ H^* f &= k'A\left\{Y_{1(0)}f_{(t)} + \int_0^t \frac{dY_{1(t-\tau)}}{d(t-\tau)}f_{(\tau)}d\tau\right\} \end{aligned} \tag{7}$$

where relaxation kernels $Y(t)$ and $Y_1(t)$ can be arbitrarily chosen depending on materials.

The boundary conditions:

$$\begin{aligned} -u_b + \hat{u}_b &= 0 \quad \text{on} \quad \Gamma_{u_b} \\ -\Omega_n + \hat{\Omega}_n &= 0 \quad \text{on} \quad \Gamma_{\Omega_n} \\ -\Omega_t + \hat{\Omega}_t &= 0 \quad \text{on} \quad \Gamma_{\Omega_t} \\ M_n - \hat{M}_n &= 0 \quad \text{on} \quad \Gamma_{M_n} \\ M_t - \hat{M}_t &= 0 \quad \text{on} \quad \Gamma_{M_t} \\ T_b - \hat{T}_b &= 0 \quad \text{on} \quad \Gamma_{T_b} \end{aligned} \tag{8}$$

where the quantities with hat are given at the boundary points. Of course these boundary conditions do not belong to a specific problem. These boundary conditions serve to include boundary terms to the functional.

In order to remove the time derivatives from governing equations and boundary conditions, the method of Laplace-Carson transform will be employed. The Laplace-Carson transform of a real function is

$$\bar{f}_{(s)} = sf_{(s)} \tag{9}$$

where the Laplace transform of a real function is

$$f_{(s)} = L[f_{(t)}] = \int_0^{\infty} e^{-st} f_{(t)} dt$$

$$f_{(t)} = L^{-1}[f_{(s)}] = \frac{1}{2\pi i}\int_{a-i\infty}^{a+i\infty} e^{st} f_{(s)} ds \tag{10}$$

The integration is carried out in the plane of the complex variable s along an infinite straight line parallel to the imaginary axis and situated so that all singular points of function $f_{(s)}$ are located to the left of this straight line.

Taking Laplace-Carson transform of Eq. (1), Eq. (2), Eq. (6) and Eq. (8), we will obtain the field equations in Laplace-Carson space;

$$-\frac{d\overline{T}_b}{d\theta} - \overline{q}R + kR\overline{u}_b = 0$$

$$-\frac{d\overline{M}_n}{d\theta} - \overline{M}_t + R\overline{T}_b - R\overline{m}_n = 0$$

$$-\frac{d\overline{M}_t}{d\theta} + \overline{M}_n - R\overline{m}_t + k_t R\overline{\Omega}_t = 0 \tag{11a}$$

$$\frac{d\overline{\Omega}_t}{d\theta} - \overline{\Omega}_n - R\overline{\omega}_t = 0$$

$$\frac{d\overline{\Omega}_n}{d\theta} + \overline{\Omega}_t - R\overline{\omega}_n = 0$$

$$\frac{d\overline{u}_b}{d\theta} + R\overline{\Omega}_n - R\overline{\gamma}_b = 0 \tag{11b}$$

$$-\overline{M}_n + \overline{D}_n^*\overline{\omega}_n = 0, \quad -\overline{M}_t + \overline{D}_t^*\overline{\omega}_t = 0, \quad -\overline{T}_b + \overline{H}^*\overline{\gamma} = 0 \tag{11c}$$

$$-\overline{u}_b + \hat{\overline{u}}_b = 0, \quad -\overline{\Omega}_n + \hat{\overline{\Omega}}_n = 0, \quad -\overline{\Omega}_t + \hat{\overline{\Omega}}_t = 0,$$

$$\overline{M}_n - \hat{\overline{M}}_n = 0, \quad \overline{M}_t - \hat{\overline{M}}_t = 0, \quad \overline{T}_b - \hat{\overline{T}}_b = 0 \tag{11d}$$

where $\overline{q}$ represents applied loads as well as dynamic effects and

$$\overline{D}_n^* = I_n\overline{Y}$$

$$\overline{D}_t^* = I_0\overline{Y_1}$$

$$\overline{H}^* = k'A\overline{Y_1} \tag{12}$$

These equations can be written in operator form similar to elastic circular beam (Aköz and Kadıoğlu 1996)

$$\boldsymbol{Q} = \boldsymbol{P}\boldsymbol{u} - \boldsymbol{f} \tag{13}$$

The explicit form of the operator is given in the Appendix. If the operator $\boldsymbol{Q}$ is potential

$$\langle d\boldsymbol{Q}(\boldsymbol{u}, \bar{\boldsymbol{u}}), \boldsymbol{u}^{*}\rangle = \langle d\boldsymbol{Q}(\boldsymbol{u}, \boldsymbol{u}^{*}), \bar{\boldsymbol{u}}\rangle \tag{14}$$

must be satisfied.

After satisfying the requirement the functional is obtained (Oden and Reddy 1976) as

$$\boldsymbol{I}(\boldsymbol{u}) = \int_0^1 \langle Q(\xi\boldsymbol{u}, \boldsymbol{f}), \boldsymbol{u}\rangle d\xi \tag{15}$$

Inserting Eq. (13) into Eq. (15) the functional for viscoelastic circular beam is obtained

$$\begin{aligned}\boldsymbol{I}(\boldsymbol{u}) = {} & \frac{1}{2}kR[\bar{u}_b, \bar{u}_b] - R[\bar{m}_t, \bar{\Omega}_t] - R[\bar{q}, \bar{u}_b] + R[\bar{T}_b, \bar{\Omega}_n] \\ & + [\bar{M}_n, \bar{\Omega}_t] - [\bar{M}_t, \bar{\Omega}_n] + [\bar{T}_b', \bar{u}_b] - [\bar{M}_n', \bar{\Omega}_n] - [\bar{M}_t', \bar{\Omega}_t] \\ & - \frac{R}{2\bar{D}_t^*}[\bar{M}_t, \bar{M}_t] - \frac{R}{2\bar{D}_n^*}[\bar{M}_n, \bar{M}_n] - \frac{R}{2\bar{H}^*}[\bar{T}_b, \bar{T}_b] \\ & + [(\bar{T}_b - \hat{\bar{T}}_b), \bar{u}_b]_\sigma + [(\bar{M}_n - \hat{\bar{M}}_n), \bar{\Omega}_n]_\sigma + [(\bar{M}_t - \hat{\bar{M}}_t), \bar{\Omega}_t]_\sigma \\ & + [\hat{\bar{u}}_b, \bar{T}_b]_\varepsilon + [\hat{\bar{\Omega}}_n, \bar{M}_n]_\varepsilon + [\hat{\bar{\Omega}}_t, \bar{M}_t]_\varepsilon \end{aligned} \tag{16}$$

where [,] is the inner product which is defined as

$$[f, g] = \int fgRd\theta \tag{17}$$

Using functional in Eq. (16) VCR12 can be obtained with six nodal variables $\bar{u}_b, \bar{\Omega}_n, \bar{\Omega}_t, \bar{M}_n, \bar{M}_t, \bar{T}_b$.

3. The finite element formulation of viscoelastic circular beams on elastic foundation

The functional variables in Eq. (16) are in Laplace space. Therefore the finite element formulation belongs to the same space. To derive the finite element formulation first the interpolation function must be chosen. The regularity of the shape function depends on the maximum degree of derivatives in the functional since the first derivative of the variables exist in the functional in Eq. (16) conforming element formulation for the shape function Ψ must satisfy the following properties. $\Psi \in C^0(\underline{\Omega})$ and $\Psi \in H'(\Gamma)$ where H' is the Sobolev space (Reddy 1986).

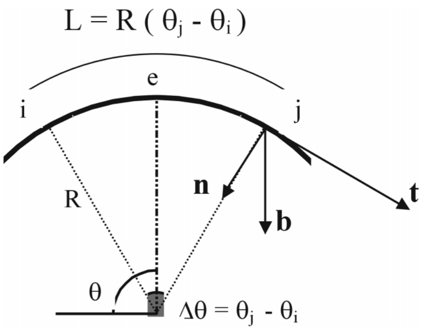

Fig. 2 Linear circular element for circular beam

The shape functions for VCR12 are

$$\Psi_i = \frac{R(\theta_i - \theta)}{L} \qquad \Psi_j = \frac{R(\theta - \theta_j)}{L} \tag{18}$$

where variable is illustrated in Fig. 2.

All known and unknown variables have been expressed by the interpolation function as follows:

$$\begin{aligned}
\bar{u}_b &= u_{bi}\Psi_i + u_{bj}\Psi_j \\
\bar{\Omega}_n &= \Omega_{ni}\Psi_i + \Omega_{nj}\Psi_j \\
\bar{\Omega}_t &= \Omega_{ti}\Psi_i + \Omega_{tj}\Psi_j \\
\bar{T}_b &= T_{bi}\Psi_i + T_{bj}\Psi_j \\
\bar{M}_n &= M_{ni}\Psi_i + M_{nj}\Psi_j \\
\bar{M}_t &= M_{ti}\Psi_i + M_{tj}\Psi_j \\
\bar{q} &= q_i\Psi_i + q_j\Psi_j
\end{aligned} \tag{19}$$

Also, to take into account variable rigidities, they will be expressed in terms of interpolation functions as

$$\begin{aligned}
\frac{1}{\bar{D}_n^*} &= X_i\Psi_i + X_j\Psi_j \\
\frac{1}{\bar{D}_t^*} &= D_i\Psi_i + D_j\Psi_j \\
\frac{1}{\bar{H}_n^*} &= A_i\Psi_i + A_j\Psi_j
\end{aligned} \tag{20}$$

All expressions of unknown and known quantities in terms of interpolation functions are inserted into Eq. (16) and after extremization of this functional with respect to twelve nodal variables the following element matrix is derived:

$$\begin{bmatrix} k_{11} & 0 & 0 & 0 & 0 & \frac{1}{2} & k_{17} & 0 & 0 & 0 & 0 & \frac{-1}{2} \\ 0 & 0 & 0 & \frac{-L}{3R} & \frac{1}{2} & \frac{L}{3} & 0 & 0 & 0 & \frac{-L}{6R} & \frac{-1}{2} & \frac{L}{3} \\ 0 & 0 & 0 & \frac{1}{2} & \frac{L}{3R} & 0 & 0 & 0 & 0 & \frac{-1}{2} & \frac{-L}{6R} & 0 \\ 0 & \frac{-L}{3R} & \frac{1}{2} & \frac{-L}{3\overline{D}_t^*} & 0 & 0 & 0 & -\frac{L}{6R} & \frac{1}{2} & \frac{-L}{6\overline{D}_t^*} & 0 & 0 \\ 0 & \frac{1}{2} & \frac{L}{3R} & 0 & \frac{-L}{3\overline{D}_n^*} & 0 & 0 & \frac{1}{2} & \frac{L}{6R} & 0 & \frac{-L}{6\overline{D}_n^*} & 0 \\ \frac{1}{2} & \frac{L}{3} & 0 & 0 & 0 & \frac{-L}{3\overline{\overline{H}}} & \frac{1}{2} & \frac{L}{6} & 0 & 0 & 0 & \frac{-L}{6\overline{\overline{H}}} \\ k_{71} & 0 & 0 & 0 & 0 & \frac{1}{2} & k_{77} & 0 & 0 & 0 & 0 & \frac{-1}{2} \\ 0 & 0 & 0 & \frac{-L}{6R} & \frac{1}{2} & \frac{L}{6} & 0 & 0 & 0 & \frac{-L}{3R} & \frac{-1}{2} & \frac{L}{3} \\ 0 & 0 & 0 & \frac{1}{2} & \frac{L}{6R} & 0 & 0 & 0 & 0 & \frac{-1}{2} & \frac{L}{3R} & 0 \\ 0 & \frac{-L}{6R} & \frac{-1}{2} & \frac{-L}{6\overline{D}_t^*} & 0 & 0 & 0 & \frac{-L}{3R} & \frac{-1}{2} & \frac{-L}{3\overline{D}_t^*} & 0 & 0 \\ 0 & \frac{-1}{2} & \frac{-L}{6R} & 0 & \frac{-L}{6\overline{D}_n^*} & 0 & 0 & \frac{-1}{2} & \frac{L}{3R} & 0 & \frac{-L}{3\overline{D}_n^*} & 0 \\ \frac{-1}{2} & \frac{L}{3} & 0 & 0 & 0 & \frac{-L}{6\overline{\overline{H}}} & \frac{-1}{2} & \frac{L}{3} & 0 & 0 & 0 & \frac{-L}{3\overline{\overline{H}}} \end{bmatrix} \begin{pmatrix} u_{bi} \\ \Omega_{ni} \\ \Omega_{ti} \\ M_{ti} \\ M_{ni} \\ T_{bi} \\ u_{bj} \\ \Omega_{nj} \\ \Omega_{tj} \\ M_{tj} \\ M_{nj} \\ T_{bj} \end{pmatrix} = \begin{bmatrix} \overline{q}_i\frac{L}{3}+\overline{q}_j\frac{L}{6} \\ 0 \\ 0 \\ 0 \\ 0 \\ 0 \\ \overline{q}_i\frac{L}{6}+\overline{q}_j\frac{L}{3} \\ 0 \\ 0 \\ 0 \\ 0 \\ 0 \end{bmatrix} \tag{21}$$

where

$$k_{11} = k_{77} = \frac{(k+\rho s^2)L}{3}$$

$$k_{17} = k_{17} = \frac{(k+\rho s^2)L}{6} \tag{22}$$

Throughout the mathematical manipulations the following properties of interpolation function are used:

$$\int_{\theta_i}^{\theta_j} \Psi_i \Psi_i d\theta = \frac{1}{3}\Delta\theta \qquad \int_{\theta_i}^{\theta_j} \Psi_j \Psi_j d\theta = \frac{1}{3}\Delta\theta$$

$$\int_{\theta_i}^{\theta_j} \Psi_i \Psi_j d\theta = \frac{1}{6}\Delta\theta \qquad \int_{\theta_i}^{\theta_j} \Psi_i \Psi_j' \, d\theta = -\frac{1}{2}$$

$$\int_{\theta_i}^{\theta_j} \Psi_j \Psi_j' \, d\theta = \frac{1}{2} \qquad\qquad \int_{\theta_i}^{\theta_j} \Psi_i \Psi_j' \, d\theta = -\frac{1}{2} \tag{23}$$

The element equations are valid for circular beam on elastic foundation with variable cross-sections. The properties of the element equations are:

- The coefficient element matrix is symmetrical
- They reduce to straight beam matrix for $R \to \infty$
- For a beam with constant cross-section $A_i = A_j$, $X_i = X_j$, $Y_i = Y_j$
- For a special case the size of matrix reduces. For straight beams the order of the matrix will be 6×6.
- The variables with hats are valid only when a corresponding boundary condition is defined.

4. Numerical inversion of FEM solutions

FEM formulation of viscoelastic circular beam is derived in Laplace-Carson space and the numerical solution is obtained for different numerical values of transform parameters. At this stage, the inverse transformation is neccessary in order to present the solution in the original domain. There exist various methods for the inverse Laplace transformation. Among these, we will restrict ourselves to the methods called numerical Laplace inversion such as Schapery, Dubner and Abate, Durbin, MDOP. The classification of Laplace inversion techniques are given by Aral and Gülçat (1977). For more information of Laplace inversion process the interested reader is referred to literature (Schapery 1962, Dubner and Abate 1968, Krylov and Skoblya 1969, Durbin 1974, Narayanan and Beskos 1982).

Schapery method is particularly suitable for the quasi-static problems for which inertia effects are neglected. In this method time dependent variable is divided into parts

$$v_{(t)} = \Delta v_{(t)} + v_{\infty}, \qquad \Delta v_{(\infty)} = 0 \tag{24}$$

First part is expressed as Dirichlet series

$$\tilde{\Delta} v_{(t)} = \sum_{i=1}^{N} A_i e^{-\lambda_i t} \tag{25}$$

The square of error approximation is

$$E^2 = \int_0^{\infty} \left[\Delta v_{(t)} - \sum_{i=1}^{N} A_i e^{-\lambda_i t} \right]^2 dt \tag{26}$$

If the error is minimized with respect to Constant A_j we have

$$\sum_{i=1}^{N} \frac{1}{1 + \dfrac{\lambda_i}{\lambda_j}} A_i = \overline{\Delta v}(s)\big|_{s = \lambda_j} \quad j = 1, N \tag{27}$$

Then, N linear equations are obtained for A_i.

$$\bar{v}_{(s)} = \overline{\Delta v}(s) + \frac{v_\infty}{s} \tag{28}$$

and inserting $s\overline{\Delta v}(s)$ into Eq. (27), we have

$$\sum_{i=1}^{N} \frac{1}{1 + \frac{\lambda_i}{\lambda_j}} A_i = (\bar{v}_{(s)} - v_\infty)\big|_{s = \lambda_j} \tag{29}$$

Where $\bar{v}_{(s)}$ is the Laplace-Carson transform of $v_{(z,\,t)}$ and is directly obtained from finite element solutions.

In the maximum degree of precisions a methods $Y_{(t)}$ can be approximated by quadrature.

$$f_{(t)} = \frac{1}{t}\sum_{k=1}^{n} W^k S_k^m \left[F\left(\frac{s_k}{t}\right)\right] \tag{30}$$

where S_k is the abcissa and W_k is the weighting function. Weighting numbers are taken from Kyrlov and Skoblya (1969). In this study calculations are carried out for $m = 1$ and $n = 10$.

In Dubner & Abate method $f_{(t)}$ is assumed to be expanded in a series of orthogonal polynomials $\Phi_{(t)}$, as

$$f_{(t)} = \sum_{k=0}^{\infty} C_k \Phi_k(t) \tag{31}$$

The coefficients C_k are then expressed in terms of the values of the $f_{(s)}$ at certain real points and we end up with

$$f_{(t)} = \frac{2e^{at}}{T}\left\{\frac{1}{2}Re[F(a)] + \sum_{k=1}^{\infty} Re\left[F\left(a + \frac{k\pi i}{T}\right]\cos\left(\frac{k\pi}{T}t\right)\right\} \tag{32}$$

If we substitude $aT = A$ and $T = 2t$ in Eq. (32) we obtain

$$f_{(t)} = \frac{e^{\frac{A}{2}}}{t}\left\{\frac{1}{2}F\left(\frac{A}{2t}\right) + \sum_{n=1}^{\infty}(-1)^n Re\left[F\left(\frac{A + 2n\pi i}{2t}\right]\right\} \tag{33}$$

In the computer programming Eq. (32) is employed. Durbin method is actually an efficient improvement of Dubner & Abate. Durbin combined both finite Fourier Sine and Cosine transforms to obtain the inversion formula

$$f_{(t_j)} = \frac{2e^{aj\Delta t}}{T}\left\{-\frac{1}{2}Re[F(a)] + Re\left[\sum_{k=0}^{N-1} L_k(A_{(k)} + iB_{(k)})\right]W^{jk}\right\} \tag{34}$$

where

$$A_{(k)} = \sum_{p=0}^{L} Re\left[F\left(a + i(k+pN)\frac{2\pi}{N}\right)\right]$$

$$B_{(k)} = \sum_{p=0}^{L} Im\left[F\left(a + i(k+pN)\frac{2\pi}{N}\right)\right]$$

$$W = \cos\left(\frac{2\pi}{N}\right) + i\sin\left(\frac{2\pi}{N}\right)$$

$$L_k = \frac{\sin\left(\frac{k\pi}{N}\right)}{\left(\frac{k\pi}{N}\right)} \tag{35}$$

Computer program was written for the above inversion methods. Results of these method are discussed in applications.

5. Applications

The performance of the method is tested through various problem presented below. In all applications Kelvin or three parameter Kelvin model is employed. These models represented by a spring-dashpot model are illustrated in Fig. 3. In the Kelvin and three parameter Kelvin models displacement approaches finite value for $t \to \infty$. A three parameter Kelvin model has elastic response for $t = 0$ but Kelvin model doesn't have elastic response. The material coefficients are chosen as in reference (Chen 1995, Aköz and Kadıoğlu 1999).

The three parameter solids: $E_1 = 98$ MPa
$E_2 = 24.5$ MPa
$\eta = 274.4$ MPa.s
$\nu = 0.3$

The Kelvin model: $E = 98$ MPa
$\eta = 27.44$ MPa.s
$\nu = 0.3$

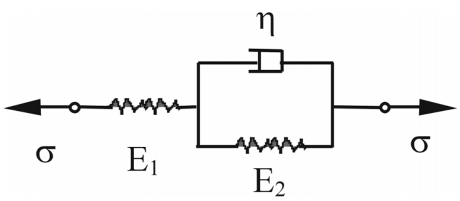

Fig. 3 The model of Three Parameter Viscoelastic Material (TPM)

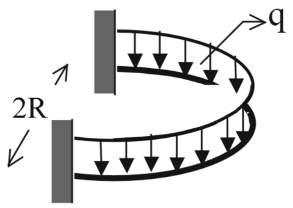

Fig. 4 Fixed-fixed semi-circular beam

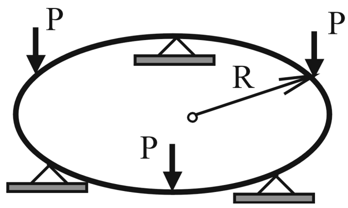

Fig. 5 Circular beam with concentraeted external loads

Relaxation moduli of Kelvin and Three parameter Kelvin material are as follows:

$$J_{(t)} = \frac{1}{E}\left(1-e^{-\frac{E}{\eta}t}\right), \qquad J_{(t)} = \frac{1}{E_1}+\frac{1}{E_2}\left(1-e^{-\frac{E_2}{\eta}t}\right) \tag{36}$$

In all applications meter (m.), seconds (s.) are used to measure the displacement and time respectively. Although a different relaxation modulus can be chosen for Shear modulus G, in these examples Poisson ratio ν is assumed as a constant. Therefore the same relaxation modulus in Eq. (36) are used to represent the shear modulus G.

Fixed ended semi-circular beam in Fig. 4 and circular beam supported on three points in Fig. 5 are solved for different loads. The time history of load in applications are illustrated in Fig. 6. In all example dimension of cross-section are taken as b = 1 m., h = 1 m. Except example 6.

Example 1: *Fixed ended semi-circular beam with type I load.*

Uniform vertical load q_0 = 10 N/m is acting vertically on the semi-circular fixed-ended beam Fig. 4. The time history of load is sketched in Fig. 6(a). This problem is solved for TPK (Three-parameter Kelvin Solid) employing MDOP, Dubner and Durbin inverse transform techniques. The displacement

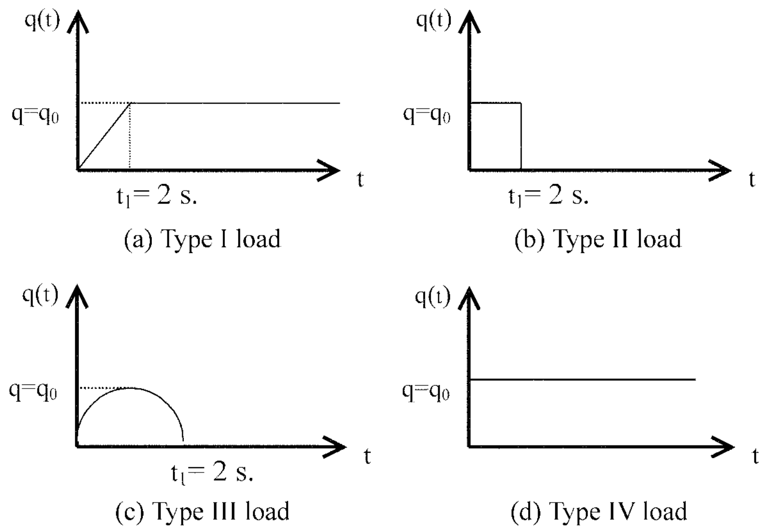

Fig. 6 Time histories of external loads

variation of center point with respect to time is depicted in Fig. 7 for $t < t_1 = 2$ s. and for $t > t_1 = 2$ s. in Fig. 8. In this problem MDOP and Durbin give perfect results. Fluctuation is observed as the time increases in Dubner inverse transform technique (for $aT = 10$, $N = 100$). Since fluctuation exist in Dubner method the results are not shown in the figure. It is experienced that if these parameters increase fluctution move to the right side on time scale.

Example 2: *Fixed ended semi-circular beam with type II load.*

In this example, the problem given in the previous example is solved for the load given Fig. 6(b). The time duration is assumed as $t_1 = 2$ s. The full time history of the displacement of center point is depicted in Fig. 9. In this problem MDOP, Dubner and Durbin inverse Laplace transform techniques are employed.

Example 3: *Fixed-ended semi-circular beam with type III load.*

In this example, the problem given in the previous example is solved for the load given in Fig. 6(c). The full the time history of the displacement of the center point is depicted in Fig. 10. In this example, Durbin gives the perfect results. The error in the solution depends on the parameter N in Durbin method. For the bigger number N error is decreases. For example if $N = 1000$ is used the correct results can be obtained up to 30 s.

Example 4: *Fixed-ended semi-circular beam with type VI load.*

In this example, the problem given in the previous example is solved for the load given in Fig. 6(d) (step load). The time variation of the displacement of the center point is depicted in Fig. 11. In this example Dubner, Durbin, MDOP and Shapery methods are employed. The numerical results almost are the same for all methods. Therefore it is diffucult to find difference between the curves for different methods and only one of them is given.

Example 5: *Dynamic response of fixed-ended semi-circular beam.*

The same beam as in the previous examples is considered. The problem is solved for the step function load $q = 10H(t)$ N/m using Dubner inverse Laplace transform technique. The material density ρ is assumed as 500 kg/m^3. The time dependent displacement at the centre of the beam for TPK solid is presented in Fig. 12. The dynamic behaviour of the viscoelastic beam disappears after $t > 25$ s. for selected materials.

Example 6: *Circular beam with concentrated loads.*

The circular beam on three point support is studied. The concentrated forces are suddenly applied at the three symmetrically located points as indicated in Fig. 5. The geometry and material properties are $R = 5$ m., $E_1 = 98$ MPa, $E_2 = 24.5$ MPa, $\eta = 274.4$ MPa.s, $b = 1$ m., $h = 0.5$ m., $P = 1H(t)$ kN.

The time dependent displacement under the load for quasi-static and dynamic cases are presented in Fig. 13. The dynamic behaviour of viscoelastic beam disappears after $t > 25$ s. for TPK material.

The effect of thickness of beam on the amplitude and frequency is shown in Fig. 14. Frequency increases with increasing thickness as expected. Also the effect of viscosity coefficient on the vibration is presented in Fig. 15. As it is observed from Fig. 15, the displacement decreases as the viscosity coefficient increases. In dynamical solution Dubner inverse Laplace transform technique gives the best result.

Example 7: *Circular beam on elastic foundation.*

The circular beam of the previous example on elastic foundation is considered. The material density ρ is 500 kg/m^3. The Winkler coefficient k is 20 kN/m. The quasi-static and dynamic deflection under load-point is depicted in Fig. 16. As is seen from that figure, the deflection is approximately one tenth of the previous example. Also, the interaction of the beam with the foundation affects the vibration shape. The quasi-static and transient response is depicted in Fig. 16.

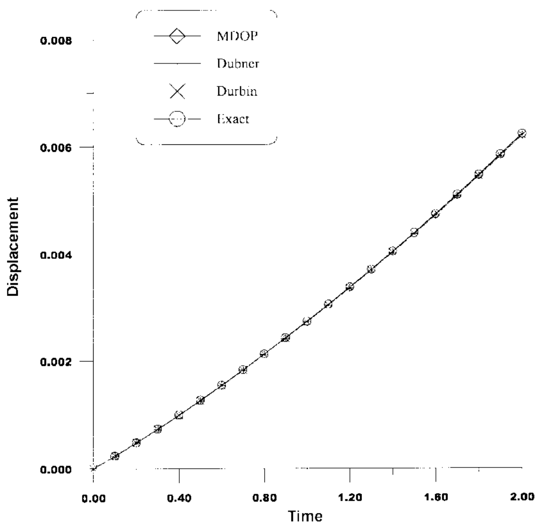

Fig. 7 Displacement variation at the centre of beam for the time load its history given in Fig. 6(a) by using MDOP, Dubner, Durbin ($t < t_1 = 2$ s.)

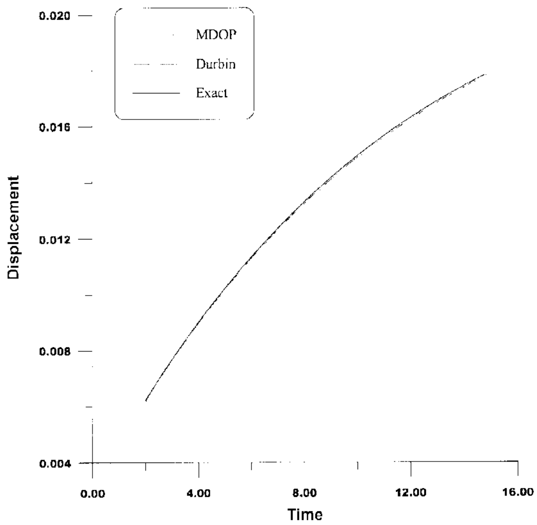

Fig. 8 The time dependent displacement at the centre of beam for the time load its history given in Fig. 6(a) ($t > t_1 = 2$ s.)

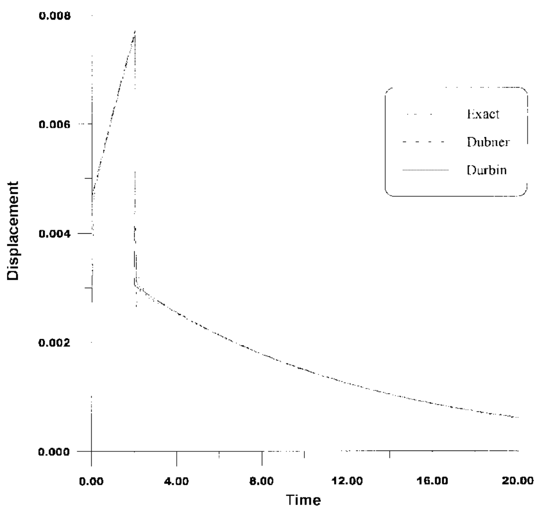

Fig. 9 The time dependent displacement at the centre of beam for the time load its history given in Fig. 6(b)

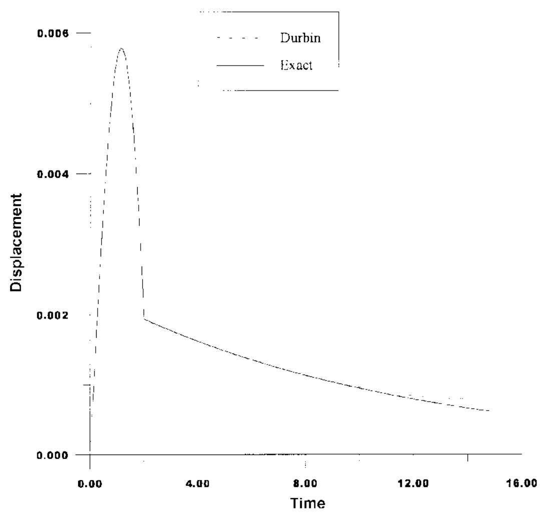

Fig. 10 The time dependent displacement at the centre of beam for the time load its history given in Fig. 6(c)

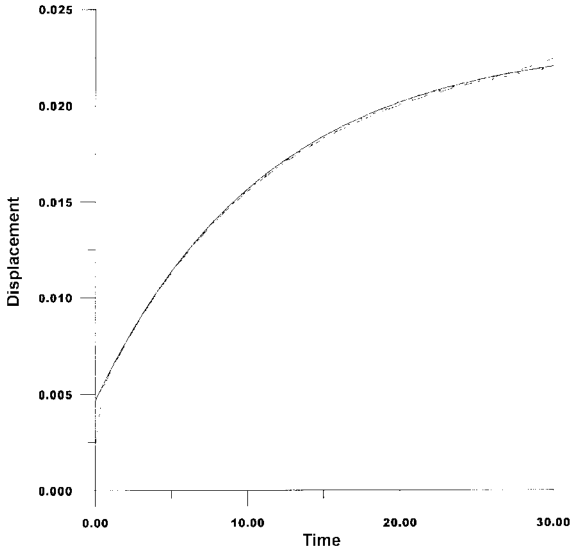

Fig. 11 Displacement variation at the centre of beam for the time load its history given in Fig. 6(d) by using MDOP, Dubner, Durbin, Schappery

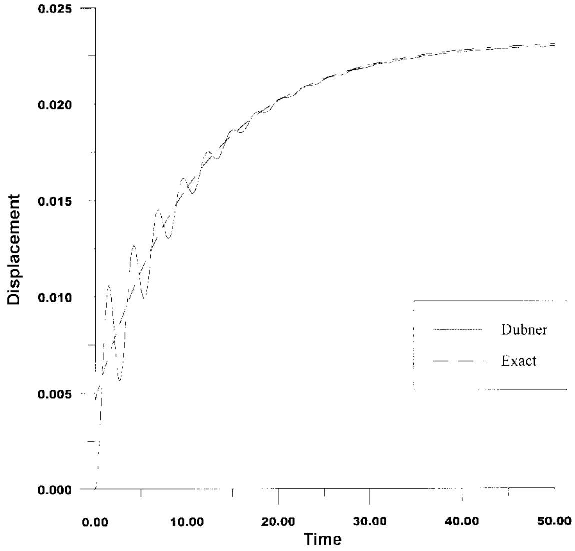

Fig. 12 The quasi-static and dynamic behaviour of the displacement at the centre of beam for TPM

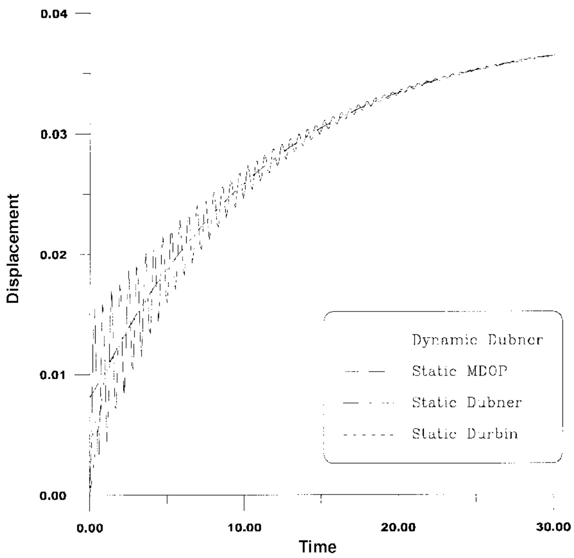

Fig. 13 The quasi-static and dynamic variation of displacement under loadpoint

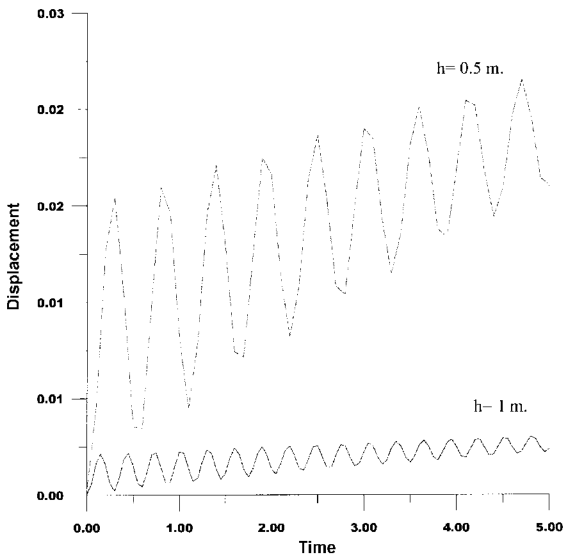

Fig. 14 The effect of thickness on the frequency and displacement

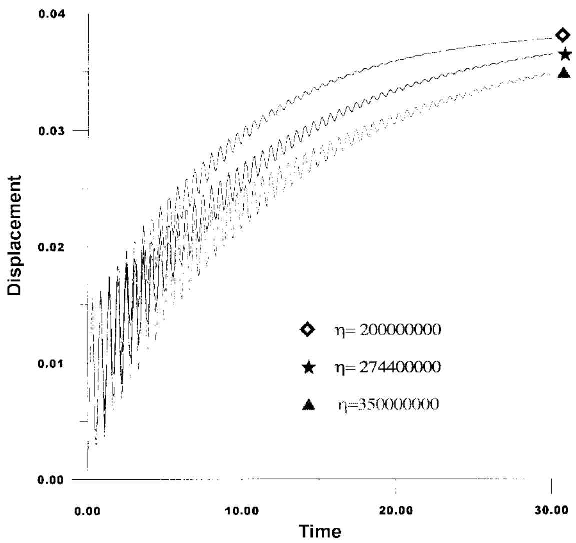

Fig. 15 The effect of viscocity coefficient on displacement

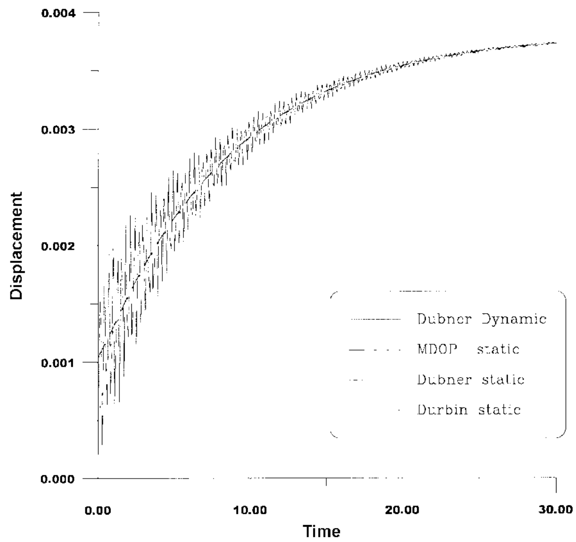

Fig. 16 The quasi-static and dynamic variation of displacement under loadpoint on elastic foundation

6. Conclusions

In this study, a finite element VCR12 developed for viscoelastic beam for circular beams on elastic foundation. To represent viscoelastic behaviour, the two constitutive relations (one for the bending and one for the shear force) in hereditary integral form are assumed. In order to remove the time derivative from governing equations and boundary conditions, the Laplace-Carson transformation is employed. A new functional is obtained for viscoelastic circular beams through systematic procedure based on Gâteaux differential which have 12 independent variables. The mixed finite element formulation VCR12 is obtained in transformed space. The Shapery, Dubner, Durbin and MDOP methods are employed for numerical inversion. The performance of the method is tested through various quasi-static and dynamic problems. The properties of this formulation briefly are:

- MDOP and Durbin method are very suitable for quasi-static problems under the constant loads. In Durbin method for much better numerical results are obtained for increasing parameters such as aT = 10, N = 100-2000.
- MDOP doesn't give the results for t = 0.
- Dubner inverse Laplace transform technique gives the best result for transient response.
- In Dubner inverse Laplace transform technique better results are obtained for increasing parameters such as aT = 10, N = 100-2000.
- It is observed that the frequency of the vibration increases with the increasing rigidity of the beam as expected.

References

Addey, R.A. and Brebbia, C.A. (1973), "Efficient method for solution of viscoelastic problem", *J. Eng. Mech.*

Div. ASCE, **99**, 1119-1127.
Aköz, A.Y. and Kadıoğlu, F. (1996), "The mixed finite element solutions of circular beam on elastic foundation", *Comput. Struct.*, **60**(4), 643-657.
Aköz, A.Y. and Kadıoğlu, F. (1999), "The mixed finite element method for the quasi-static and dynamic analysis of viscoelastic Timoshenko beams", *Int. J. Numer. Methods Eng.*, **44**, 1909-1932.
Aköz, A.Y., Omurtag, M.H. and Doğruoğlu, A. (1991), "The mixed finite element formulation for three-dimensional bars", *Int. J. Solids Structures*, **28**(2), 225-234.
Aral, M.M. and Gülçat, Ü. (1977), "A finite element Laplace transform solution technique for wave equation", *Int. J. Numer. Methods Eng.*, **11**, 1719-1732.
Chen, T. (1995), "The hybrid Laplace transform/finite element method applied to the quasi-static and dynamic analysis of viscoelastic Timoshenko beams", *Int. J. Numer. Methods Eng.*, **38**, 509-522.
Christensen, R.M. (1982), *Theory of Viscoelasticity*, 2nd ed., Academic Press, New York.
Dubner, H. and Abate, J. (1968), "Numerical inversion of Laplace transforms by relating them to finite Fourier cosine transform", *Journal of the Association for Computing Machinery,* **15**(1), 115-123.
Durbin, F. (1974), "Numerical inversion of Laplace transforms: an efficient improvement to Dubner and Abate's method", *The Computer Journal*, **17**(4), 371-376
Findley, W.N., Lai, J.S. and Onaran, K. (1976), *Creep and Relaxation of Nonlinear Visco-elastic Materials*, North-Holland, New York.
Flügge, W. (1975), *Viscoelasticity*, 2nd ed., Springer, Berlin, Heidelberg.
Hetenyi, M. (1946), *Beams on Elastic Foundation*, The University of Michigan Press, Ann Arbor, Michigan.
Johnson, A.R., Tessler, A. and Dambach, M. (1997), "Dynamics of thick viscoelastic beams", *Journal of Engineering Materials and Technology,* **119**, July, 273-278.
Kadıoğlu, F. (1999), "Quasi-static and dynamic analysis of viscoelastic beams", Ph.D. thesis (in Turkish), Department of Civil Engineering, Istanbul Technical University.
Krylov, V.I. and Skoblya, N.S. (1969), *Handbook of Numerical Inversion of Laplace Transforms*, Jeruselam by ISST Press, Wiener Bindery Ltd.
Miranda, C.K. and Nair, K. (1966), "Finite beams on elastic foundations", *J. Struct. Div.*, ASCE, **92**, 131-142.
Narayanan, G.V. and Beskos, D.E. (1982), "Numerical operational methods for time-dependent linear problems", *Int. J. Numer. Methods Eng.*, **18**, 1829-1854.
Oden, J. and Reddy, J.N. (1976), *Variational Methods in Theoretical Mechanics*, Springer, Berlin.
Rabbatnow, Yu. N. (1980), *Element of Hereditary Solid Mechanics*, Mir Publishers-Moscow.
Reddy, J.N. (1986), *Applied Functional Analysis and Variational Method in Engineering*, McGraw-Hill.
Schapery, R.A. (1962), "Approximate methods of transform inversion for viscoelastic stress analysis", *Proc. the Fourth U.S. National Congress of Applied Mechanics*, **2**, Pergamon Press, Oxford, London, New York, Paris, June, 18-21.
Ting, B.Y. and Mockry, E.F. (1983), "Beam on elastic foundation finite element", *J. Appl. Mec.*, ASCE, **109**(6), 1390-1402.
Wang, C.M., Yang, T.Q. and Lam, K.Y. (1997), "Viscoelastic Timoshenko beam solutions from Euler-Bernoulli solutions", July, 746-748.
White, J.L. (1986), "Finite element in linear viscoelasticity", *Proc. 2nd Conf. on Matrix Method in Structural Mechanics,* AFFDL-TR-68-150, 489-516.

Notation

T, M	: Shear force and bending moment.
q	: External force.
R	: Radius of circular beam.
k	: Winkler coefficient.
γ	: Shear.
Ω, ω	: Bending rotation and bending unit rotation.
A, k'	: Area of cross-section, shear coefficient.

u_i : Displacements.

D_n^*, D_t^*, H^* : Bending, torsional and shear rigidity operators of viscoelastic beam.

E, G : Young modulus and shear modulus.

ν : Poisson ratio.

$Y(\tau)$, $Y_1(\tau)$: Relaxation kernels for normal and shear stress respectively.

$J(t)$, $J_1(t)$: Creep kernels for normal and shear strain.

s : Laplace transform parameters.

t : Time.

ρ : Density.

$\overline{F}_{(s)}$: Laplace-Carson transform of any $F_{(t)}$ function.

$\boldsymbol{Q}$: Operator.

$\boldsymbol{I}(\overline{\boldsymbol{u}})$: Functional.

$[f, g]$: Inner product in Laplace-Carson space.

$[\ ,\ ]_\sigma$: Valid at the point where dynamic conditions are given.

$[\ ,\ ]_\varepsilon$: Valid at the point where geometric conditions are given.

$\langle\ ,\ \rangle$: Inner product

Appendix

The operator form at field equation in Laplace-Carson space is:

$$
\begin{vmatrix}
kR & 0 & 0 & 0 & 0 & -\frac{d}{d\theta} & 0 & 0 & 0 & 0 & 0 & 0 & 0 & 0 & 0 \\
0 & 0 & 0 & 0 & -\frac{d}{d\theta} & R & 0 & 0 & 0 & 0 & 0 & 0 & 0 & 0 & 0 \\
0 & 0 & 0 & -\frac{d}{d\theta} & 1 & 0 & 0 & 0 & 0 & 0 & 0 & 0 & 0 & 0 & 0 \\
0 & -1 & \frac{d}{d\theta} & 0 & 0 & 0 & -R & 0 & 0 & 0 & 0 & 0 & 0 & 0 & 0 \\
0 & \frac{d}{d\theta} & 1 & 0 & 0 & 0 & 0 & -R & 0 & 0 & 0 & 0 & 0 & 0 & 0 \\
\frac{d}{d\theta} & R & 0 & 0 & 0 & 0 & 0 & 0 & -R & 0 & 0 & 0 & 0 & 0 & 0 \\
0 & 0 & 0 & -1 & 0 & 0 & \overline{D}_t^* & 0 & 0 & 0 & 0 & 0 & 0 & 0 & 0 \\
0 & 0 & 0 & 0 & -1 & 0 & 0 & \overline{D}_n^* & 0 & 0 & 0 & 0 & 0 & 0 & 0 \\
0 & 0 & 0 & 0 & 0 & -1 & 0 & 0 & \overline{H}^* & 0 & & 0 & 0 & 0 & 0 \\
0 & 0 & 0 & 0 & 0 & 0 & 0 & 0 & 0 & 0 & 0 & 0 & 0 & 0 & 1 \\
0 & 0 & 0 & 0 & 0 & 0 & 0 & 0 & 0 & 0 & 0 & 0 & 0 & 1 & 0 \\
0 & 0 & 0 & 0 & 0 & 0 & 0 & 0 & 0 & 0 & 0 & 0 & 1 & 0 & 0 \\
0 & 0 & 0 & 0 & 0 & 0 & 0 & 0 & 0 & 0 & 0 & -1 & 0 & 0 & 0 \\
0 & 0 & 0 & 0 & 0 & 0 & 0 & 0 & 0 & 0 & -1 & 0 & 0 & 0 & 0 \\
0 & 0 & 0 & 0 & 0 & 0 & 0 & 0 & 0 & -1 & 0 & 0 & 0 & 0 & 0
\end{vmatrix}
\cdot
\begin{vmatrix}
\overline{u}_b \\ \overline{\Omega}_n \\ \overline{\Omega}_t \\ \overline{M}_t \\ \overline{M}_n \\ \overline{T}_b \\ \overline{\omega}_t \\ \overline{\omega}_n \\ \overline{\gamma}_b \\ \overline{u}_{b0} \\ \overline{\Omega}_{n0} \\ \overline{\Omega}_{t0} \\ \overline{M}_{t0} \\ \overline{M}_{n0} \\ \overline{T}_{b0}
\end{vmatrix}
=
\begin{vmatrix}
qR \\ 0 \\ 0 \\ 0 \\ 0 \\ 0 \\ 0 \\ 0 \\ 0 \\ \hat{\overline{T}}_{b0} \\ \hat{\overline{M}}_{n0} \\ \hat{\overline{M}}_{t0} \\ -\hat{\overline{\Omega}}_{t0} \\ -\hat{\overline{\Omega}}_{n0} \\ -\hat{\overline{u}}_{b0}
\end{vmatrix}
$$